Diabetologia (1991) 34: 469–476
0012186X91001443

Diabetologia

Changes in vitreal oxygen tension distribution in the streptozotocin diabetic rat

V. A. Alder, D.-Y. Yu, S. J. Cringle and E.-N. Su

Lions Eye Institute and Department of Surgery, University of Western Australia, Nedlands, Western Australia, Australia

Summary. Measurements of vitreal oxygen tension have been made for the first time in the streptozotocin-induced diabetic rat eye. A total of 36 Sprague Dawley rats were divided into a control ($n = 18$) and streptozotocin injected group ($n = 18$), and after 5–6 weeks of established hyperglycaemia, an acute experiment was performed in which vitreal oxygen tension profiles were determined with oxygen sensitive microelectrodes. The control rats had significant oxygen tension gradients in the vitreous close to retinal arteries with relatively flat oxygen tension profiles close to retinal veins and intermediate regions. All control rats had a substantial arteriovenous oxygen tension difference when measurements were made on retinal arteries and veins. In contrast the oxygen tension profiles measured in the vitreous of streptozotocin rats showed markedly reduced oxygen gradients in the vicinity of retinal arteries and a smaller arteriovenous oxygen tension difference. In both groups of rats, for distances of 500 μm and greater from the retina (mid vitreous) a plateau oxygen tension value was observed. No significant difference was found in this mean mid vitreous value between the control rats and diabetic rats under the same systemic conditions. We conclude that there are significant changes in oxygen tension near retinal arteries in streptozotocin-induced diabetes before any histopathological changes are evident.

Key words: Diabetes mellitus, streptozotocin, rat, oxygen, eye, vitreous, microelectrodes.

The sequence of pathophysiological events which occurs early in diabetic retinopathy and leads ultimately to the irreversible stage of capillary non-perfusion, tissue ischaemia and neovascularisation is only partly understood. The classical description of the normal vascular bed of the human retinal circulation [1–2] and the observed pathological changes in diabetes mellitus [3] were due to Kuwabara and co-workers. They introduced the technique of flat mounting a trypsin digest of the retina to provide a pseudo three-dimensional picture of the major components of the retinal circulation and demonstrated that the earliest detectable alterations to the microvasculature of the retina in diabetic retinopathy are pericyte loss and basement membrane thickening. At a much later stage ghost vessels and microaneurysms are observed [3]. A large amount of histological data has subsequently been accumulated from human tissue and animal models of induced diabetes which support these original conclusions [4–9]. In parallel with these structural alterations there is evidence for concomitant functional changes with an early reduction in the integrity of the blood retinal barrier which probably occurs initially at the level of the retinal pigment epithelial cells [10–16]. Added to this is the data demonstrating that erythrocyte properties are affected directly in response to the induced hyperglycaemia, so that blood volume expands, and glycosylation of haemoglobin and other blood proteins leads to an increase in erythrocyte fragility and a decrease in deformability [17–21]. These changes can be expected to affect the dynamics of blood flow through the capillaries, indeed there is some evidence that with advanced retinal vascular disease the perfusion of capillaries by erythrocytes is reduced [22]. Furthermore, there is an accompanying change of the oxyhaemoglobin dissociation curve resulting in an increased affinity of haemoglobin for oxygen and a consequent reduction in the offloading capability for oxygen in response to tissue demands [17]. Some of these parameters are observed to change very early in diabetes and this raises the possibility that alterations in oxygen distribution and consumption play an early and critical role in the pathology. Coupled with these observations is data showing that the capacity of the retinal circulation to autoregulate its blood flow in response to tissue demands is impaired in diabetes [23–24]. Mean circulation time has been shown to increase [25], and at the stage where overt

diabetic retinopathy is present blood velocity is decreased, but vessel diameter is increased so that retinal blood flow is normal [26]. This reduction in autoregulatory capacity for a circulation which normally operates with a very large arteriovenous oxygen tension difference and which relies heavily on local vascular autoregulation to ease its way out of difficulties puts inner retinal tissue particularly at risk from hypoxia in diabetes.

We have investigated the possibility of alterations in retinal oxygen distribution in very early diabetes by comparing oxygen tension distribution in the vitreous of normal and streptozotocin (STZ)-induced diabetic rats after only 5–6 weeks of hyperglycaemia.

Materials and methods

Animals

Male Sprague Dawley rats aged 10–11 weeks were randomly assigned into two groups, the first was an age-matched control group ($n = 18$) and the second group ($n = 18$) were given an intraperitoneal injection of streptozotocin (STZ): 50 mg/kg from a 50 mg/ml solution in sterile water. Initial body weights (Wt_i) and blood glucose levels on assignment were 354 ± 10 g (mean and SEM) and 352 ± 13 g, and 6.15 ± 1.07 and 5.85 ± 0.52 mmol/l for the control and STZ groups respectively. Diabetes was confirmed (blood glucose > 22 mmol/l) by measurements of blood glucose (measured as a non-fasting mid-morning value with blood obtained from a tail nick) (Ames glucometer, model 5529, Elkhart, Ind., USA) and observation of polyurea. Blood glucose was monitored daily for the first week post-injection to establish that hyperglycaemia eventuated. Body weight and blood glucose were subsequently measured weekly to confirm weight gain and continued hyperglycaemia. The rats (two per cage) were housed in plastic containers on sawdust with a light dark cycle 12 h/12 h. Ambient light levels averaged 290 lux. Rats were fed standard laboratory rat chow with water ad libitum. Five to six weeks after group assignment and induction each rat underwent an acute experiment to measure vitreal oxygen tension distribution. Body weight of both groups increased after induction however, the final weight (Wt_f) was significantly less in the STZ group (387 ± 10 g) than in the control group (441 ± 15 g), $p = 0.005$. The STZ rats were not treated with insulin.

General surgery

Rats were anaesthetized with an intraperitoneal injection of Inactin (Byk Gulden, Konstanz, FRG), 100 mg/kg and atropine sulphate (0.05 mg/kg) was administered to minimise salivation. The trachea was cannulated for artificial respiration (Harvard rodent respirator, model 683, South Natic, Mass., USA), with a respiratory rate of 90 per min, and tidal volume selected according to body weight from the Harvard ventilation graph [27]. Initially the rat was respired on 20% O_2, 80% N_2. The jugular vein was cannulated for insertion of a venous infusion line and the femoral artery for blood pressure monitoring (Hewlett Packard 1280C and 78905A, Waltham, Mass., USA). The rat was mounted prone in a stereotaxic frame (model 51400, Stoelting Co., Wood Dale, Ill., USA) which had been modified to hold the piezoelectric microdrive on the positioning arcs so that the microelectrode could be pivoted about the entry point into the eye. The head was fixed with respect to standard stereotaxic co-ordinates by means of ear bars. Rectal temperature was monitored with a thermistor probe and maintained between 37°C and 38°C with an infra red lamp. Blood samples (0.25 ml) were taken at selected times during the course of the experiment for arterial blood gas analysis (166 micro, Corning, Essex, UK), these samples were re-injected into the rat via the femoral artery. A continuous recording of blood pressure, end tidal CO_2 (Model 864, Beckman, Fullerton, Calif., USA), rectal temperature and vitreal oxygen tension was made on a chart recorder.

Table 1. Mean animal parameters at induction (i) and at the time of the final experiment (f) 5–6 weeks later, for the control group, the streptozotocin (STZ) group given extra ventilation STZ (N), and the systemically hypoxic group STZ (H) which were ventilated according to actual body weight

Parameter	Control	STZ (N)	STZ (H)
Wt_i (g)	354 ± 10 (18)	360 ± 17 (8)	348 ± 8 (10)
Wt_f (g)	441 ± 15 (18)	391 ± 16 (8)	382 ± 13 (10)
BG_i (mmol/l)	6.15 ± 1.07 (18)	6.01 ± 0.53 (8)	5.72 ± 0.52 (10)
BG_f (mmol/l)	6.02 ± 1.16 (18)	> 22 (8)	> 22 (10)
BP (mm Hg)	105 ± 5 (17)	112 ± 7 (8)	90 ± 6 (10)
P_aO_2 (mm Hg)	83.7 ± 2.8 (18)	90.3 ± 2.2 (8)	57.6 ± 5.9 (7)
P_aCO_2 (mm Hg)	35.8 ± 1.4 (18)	32.4 ± 3.0 (8)	42.9 ± 1.1 (7)
pH	7.382 ± 0.012 (18)	7.409 ± 0.012 (8)	7.367 ± 0.026 (7)

Wt = body weight, BG = blood glucose, BP = blood pressure, and P_aO_2, P_aCO_2, and pH = the measured blood gas parameters. The number of animals in each group is shown in parentheses

After performing experiments on the first 10 STZ rats it became apparent that setting respiratory parameters according to body weight resulted in systemic arterial hypoxia. We designated this group STZ (H), the "H" representing hypoxia. We then changed our protocol in order to rule out the effects of systemic hypoxia. The second group of STZ rats (eight rats) were ventilated with a tidal volume appropriate to the mean weight of the age-matched control rats, i.e. their expected weight had they not been made diabetic. These rats achieved normal blood gas values (normoxia) and were designated STZ (N) (see Table 1). In no case was it necessary to breath the STZ rats with a hyperoxic mixture to achieve normal blood gas values.

Ocular surgery

The pupil of the left eye was dilated (1% Mydriacyl, Alcon, Brookvale, NSW, Australia). The upper eyelid was partially removed. The eye was immobilized by suturing an eye ring to the conjunctiva at the limbus, and fixing the eye ring to the stereotaxic frame. A 1.2 mm wide incision was made through the sclera at or near pars plana ciliaris (approximately 2 mm posterior to the limbus) in the superior region using a diamond knife, taking care to avoid damage to the larger vessels or posterior lens capsule. The oxygen microelectrode was then placed through this entry hole into the vitreous body under microscope observation.

Electrode manufacture and calibration

Oxygen sensitive microelectrodes were manufactured in the laboratory by soldering a 2 cm length of 25 µm Pt/Rh wire (PT005114/8, Goodfellows Metals, Cambridge, UK) to a 20 cm length of 100 µm diameter copper wire which was threaded into a borosilicate glass capillary (inner diameter = 230 µm, outer diameter = 420 µm). The Pt/Rh tip was etched to a fine point 1–5 µm in diameter. The glass was pulled to a point at the metal tip using an electrode puller resulting in full insulation except at the tip. The final electrode tip diameter was 1–5 µm, with an exposed length of Pt/Rh of approximately 5 µm. Electrodes were biased at −0.7 V with respect to a reference electrode (Ag/AgCl) placed subcutaneously at the central vertex and the oxygen generated current was measured using a picoammeter (480 Pico, Keithley, Cleveland, Ohio, USA). Electrochemical reduction of oxygen at the electrode tip generates a current which is proportional to the oxygen tension in the medium surrounding the tip. Electrodes were calibrated before and after all experi-

ments in 0.9% NaCl equilibrated with N_2, 21% O_2 or 100% O_2 at 37°C to ensure a satisfactory oxygen response and a N_2 current close to zero. The calibration factor for the oxygen electrode was determined by equating to oxygen current in air equilibrated 0.9% NaCl to the PO_2 of this 0.9% NaCl measured with the blood gas analyser. Linearity of response between these three calibration points was assumed. Non-membranized electrodes are susceptible to protein poisoning and stirring effects. We found that immediately after measurements made in the vitreous, the calibration current in air equilibrated 0.9% NaCl was lower that the pre-experimental calibration value and that this current gradually rose to within 5% of its pre-experimental value over about 20 min. This phenomenon has also been observed by Duling Kuschinsky and Wahl [28], who found reduced calibration currents after measurements made in plasma. Their calibration currents also gradually returned to the original values on return to 0.9% NaCl. They interpreted the initial post-experiment calibration value as the true value in plasma and we have adopted the same procedure. Experiments established that this reduction in electrode sensitivity in vitreous was complete within a few minutes of electrode placement within the eye, after which the electrode current stabilized so that rarely did any noticeable drift occur during the remainder of the experiment.

Electrode manipulation in the eye

All electrode manipulation was performed using a computer controlled piezoelectric microstepper (model 6200, Burleigh Inc., New York, USA). The electrode supporting section of the stereotaxic frame was modified to take the microstepper, ensuring that the forward drive and two orientation arcs remained centred on the ocular entry hole in the sclera. The oxygen microelectrode was inserted through this hole to enter the very small [29] vitreous body. The microelectrode was then reoriented through about 60° so that as it was advanced through the vitreous, contact with the posterior capsule of the large lens [30] was avoided. A plano-concave contact lens on the cornea allowed the vitreous body and the fundus to be visualised using an operating microscope.

Oxygen measurements

The microelectrode was oriented and advanced to just touch a retinal artery, vein or an intermediate location (one in which no arterioles or venules were apparent). Most measurements were performed in the inferior retina 3 disk diameters from the optic disk. This location was preferred because it provided a clear view of the fundus in the control and STZ rats despite the minor lens changes that were evident in the STZ group. After location of the microelectrode at the retinal surface a vitreal PO_2 profile was measured in which all electrode movements and data acquisition were under computer control (Epson PC AX3, Suwa, Japan). A user written programme controlled the electrode movements and simultaneously accessed and processed the PO_2, blood pressure and rectal temperature readings using a data acquisition board (RTI815, Analog Devices, Norwood, Mass., USA). For a vitreal PO_2 profile, readings of PO_2 were taken initially every 10 µm, for a distance of 200 µm, and then in 50 µm steps for a further distance of 800 µm. The microelectrode direction was then reversed and an inserting PO_2 profile was measured at the same distance from the retinal surface. The microelectrode current was allowed a stabilisation time of 2 s at each location before the oxygen tension current was measured. In some animals the effect of increasing the percentage of inspired oxygen on vitreal PO_2 was then determined. The electrode was withdrawn to a distance of 500 µm from the intermediate location and ventilatory oxygen concentration was increased to 100% O_2. After allowing 5 min for equilibration, the electrode was advanced to touch the retina at the intermediate location and a PO_2 profile was measured. PO_2 profiles at the original arterial and venous locations were measured for direct comparison with those measured for 20% O_2 breathing. In a few experiments the effect of acute systemic hypoxia on vitreal PO_2 profiles in normal rats was determined to ascertain whether the changes occuring in the STZ rats could be mimicked by systemic hypoxia. The starting positions of all profiles were recorded by fundus drawings and sometimes by fundus photography. All experiments were performed in photopic conditions. Experiments lasted up to 9 h after which the rat was killed with an anaesthetic overdose.

Statistical analysis

All averaged values in this paper are quoted as means ± SEM. Group comparisons are performed using Student's t-test for unequal unpaired groups. The p-value quoted is the exact two-tailed value. A p-value < 0.05 is the criterion for significance.

Results

General

The means and SEM of the measured systemic parameters for the control and the two STZ groups are shown in Table 1. Wt_i and BG_i are the body weight and blood glucose values on induction to the experiment, whereas Wt_f and BG_f are the equivalent final values at the time of the acute experiment. Blood pressure, pH, P_aO_2 and P_aCO_2 are arterial blood values measured during the acute experiment. It is apparent that there was no significant difference in body weight and blood glucose at induction. However, as already stated by the time of the acute experiment body weight was significantly less in both STZ groups and blood glucose was elevated to greater than 22 mmol/l. During the acute experiment there was no significant difference between blood pressure, arterial blood gases, and pH between the control group and the STZ (N) group ventilated with the higher tidal volume. However, the STZ (H) group, ventilated according to actual body weight, was significantly hypoxic ($p < 0.0001$) with a mean P_aO_2 of 57.6 ± 5.9, and hypercapnic ($p = 0.006$) with a mean P_aCO_2 of 42.9 ± 1.1 when compared to the equivalent values for the control group. If the same systemic parameters are compared for the STZ (N) and STZ (H) groups, P_aO_2, P_aCO_2 and blood pressure were significantly different $p < 0.0001$, $p = 0.008$ and $p = 0.03$ respectively.

We consistently observed differences in the fundus appearance between the normal and STZ rats. Our normal rats had a transparent retina whereas that of the STZ-treated animals was significantly more pink in the posterior pole.

Oxygen measurements

Three typical sets of vitreal PO_2 profiles measured for 20% O_2 breathing are compared in Figures 1 a, b, and c for a control, STZ (N), and STZ (H) rat respectively. In these graphs the ordinate shows the PO_2 in mm Hg plotted as a function of distance in µm from the touching point on the retinal surface. All three are plotted on the same scales to allow easy comparison. The advancing and withdrawing

profiles are so similar in each case that only the withdrawal profile is plotted. In each Figure three profiles are shown; these are measured with the starting retinal touching location either at a retinal artery (full line), vein (dashed line) or an intermediate location (dotted line). For the control rat (Fig. 1 a) a steep gradient exists from the retinal artery with PO_2 falling from 62 mm Hg at the touching point on the artery to a plateau value of 27 mm Hg by a distance of 500 μm from the retinal surface after which there is little further change in PO_2. The venous and intermediate touching values are 24 mm Hg and 19 mm Hg. These two profiles are relatively flat, and all three profiles reach a similar plateau mid vitreous PO_2. The arteriovenous oxygen tension difference at the touching location is 38 mm Hg (from 62 mm Hg to 24 mm Hg). In order to compare vitreal profiles from different animals, including those for which absolute electrode calibrations were not known, we defined arithmetic ratios relating the PO_2 values at these touching locations (artery A, Vein V and intermediate I) and mid vitreal (MV) PO_2. This latter value is defined to be the mean PO_2 for the artery, vein and intermediate profile measured 500 μm from the retinal surface, a location where the PO_2 has already stabilised to the plateau value. For the data of Figure 1 a A/MV = 62/27 or 2.30, V/MV = 0.89, I/MV = 0.7 and A/V = 2.6. For all 18 control animals vitreal PO_2 profiles were qualitatively similar, all showed PO_2 gradients in the vicinity of an artery, all had a plateau mid vitreous value and all had a substantial arteriovenous oxygen tension difference. The means and SEM for these defined ratios, and the mean mid vitreous value for all control animals are given in Table 2.

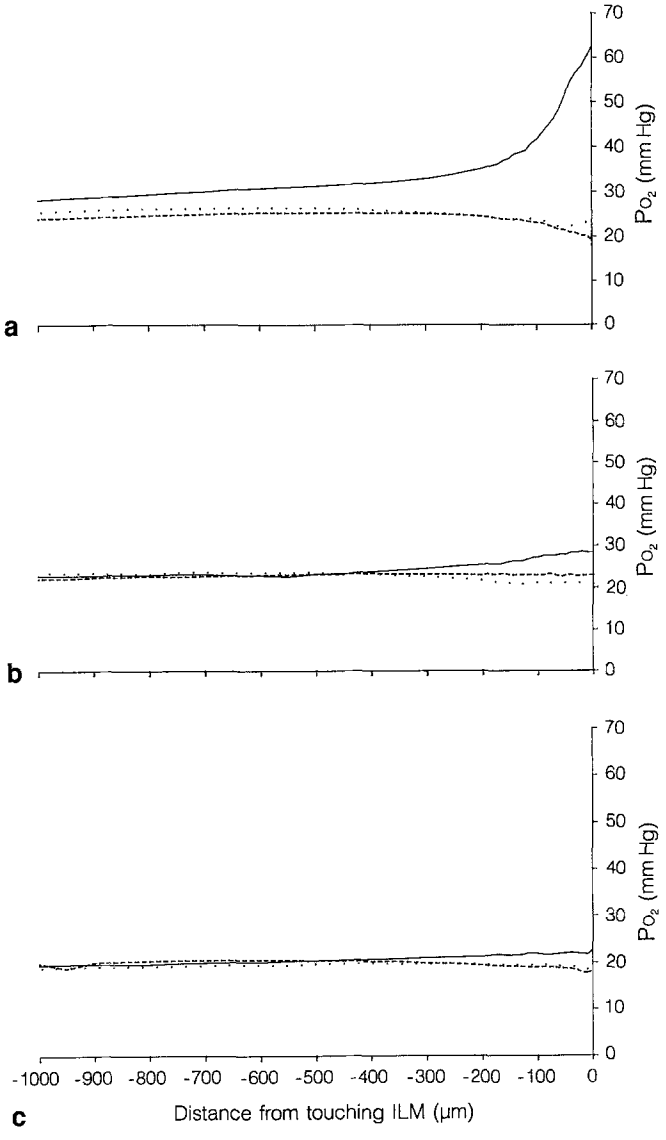

Fig. 1 a–c. Vitreal oxygen tension (PO_2) profiles for air breathing in: **a**) control rat, **b**) normoxic streptozotocin rat STZ (N) and **c**) hypoxic streptozotocin rat STZ (H). PO_2 in mm Hg is plotted as a function of distance in μm from the retinal surface, for an artery (full line), vein (dashed line) and intermediate (dotted line) touching location. ILM = Internal limiting membrane

Table 2. Summary of the mean ratios of touching oxygen tension (PO_2) at a retinal artery (A), vein (V), and intermediate location (I), compared to the plateau value (MV) 500 μm from the retina in each of the three groups. The number of animals in each group is shown in parentheses

Parameter	Control	STZ (N)	STZ (H)
PO_2 (MV)	26.4 ± 2.0 (12)	24.2 ± 1.8 (7)	20.4 ± 1.2 (7)
A/MV	1.62 ± 0.04 (17)	1.35 ± 0.10 (8)	1.10 ± 0.04 (10)
V/MV	0.98 ± 0.02 (17)	0.97 ± 0.04 (8)	0.97 ± 0.02 (10)
I/MV	0.95 ± 0.05 (17)	1.000 ± 0.05 (8)	0.99 ± 0.02 (10)

The equivalent data obtained from both groups of STZ rats was very different to that from the controls. In Figure 1 b the arterial, venous and intermediate PO_2 profiles are plotted for one STZ (N) rat. Immediately evident is the reduced PO_2 gradient close to the retina for the arterial profile. Touching PO_2 values for all three profiles are similar lying between 28 mm Hg for artery and 21 mm Hg for vein with a mid vitreous PO_2 for all three profiles of 23 mm Hg. The arteriovenous oxygen tension difference is only 7 mm Hg. It was so surprising to find minimal PO_2 gradients in the vicinity of arteries that the electrode was relocated several times and other retinal arteries checked to confirm that this was indeed a feature of the STZ rat. All vitreal PO_2 profiles measured in STZ rats showed this reduction in PO_2 gradient at the retinal artery. The mean ratio A/MV, see Table 2, for the eight STZ (N) rats was 1.35 ± 0.10 which was significantly different from that for the control group ($p = 0.006$). The other ratios A/MV and I/MV however, were close to unity and were not significantly different from that of the control rats and neither was the mid vitreal PO_2 at 24.2 ± 1.8 mm Hg. The vitreal PO_2 profiles for the STZ (H) group which are plotted in Figure 1 c were even more abnormal. The arterial profile was almost flat; touching PO_2 value was 22 mm Hg, whereas mid vitreal PO_2 was 20 mm Hg and the arteriovenous oxygen tension difference was only 3 mm Hg. The mean A/MV ratio was 1.10 ± 0.04 which was significantly different from that for the STZ (N) group, $p = 0.02$, as well as that for the control group, $p < 0.0001$. The mean mid vitreal PO_2 of 20.4 ± 1.2 mm Hg was significantly less, $p = 0.04$ than that of the control group. This important difference in arterial PO_2 profiles between the three groups of rats is shown in Figure 2 where the mean and SEM of all normalized profiles are compared, the control profiles

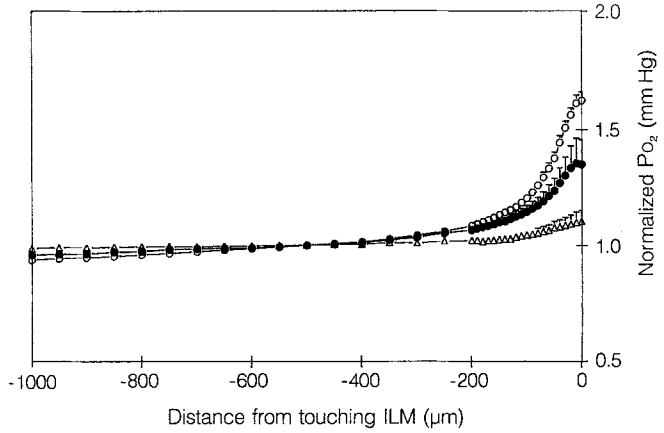

Fig. 2. Mean (±SEM) arterial oxygen tension profiles in, control rats *(open circles)*, normoxic streptozotocin rats STZ (N) (filled circles) and hypoxic streptozotocin rats STZ (H) *(open triangles)*, plotted as a function of distance in μm from the retinal surface. The data is normalised to the 500 μm point in each profile before averaging. Note the marked difference in oxygen tension gradients near retinal arteries in the three groups. ILM = Internal limiting membrane

being plotted as open circles, the STZ (N) group being shown as filled circles and the STZ (H) group being plotted as open triangles.

The effect of changing ventilation gases from air breathing to 100% O_2 breathing on the vitreal PO_2 profiles for a rat from the STZ (N) group is shown in Figure 3. Four PO_2 profiles are plotted in this figure; the lower two being arterial (full line) and venous profiles (dashed line) for air breathing, and the upper two the repeated profiles at the same locations for 100% O_2 breathing. The air breathing profiles are very similar to those of Figure 1 b, although from a different animal, and demonstrate again the minimal oxygen tension gradient in the vicinity of the retinal artery, the small arteriovenous oxygen tension difference and the plateau mid vitreous PO_2. The effect of 100% inspired oxygen is to raise all PO_2 values in the vitreous. PO_2 gradients from the retinal artery become much more apparent, and the arteriovenous oxygen tension difference is much larger than for air breathing. With 100% O_2 ventilation there is still a plateau mid vitreous

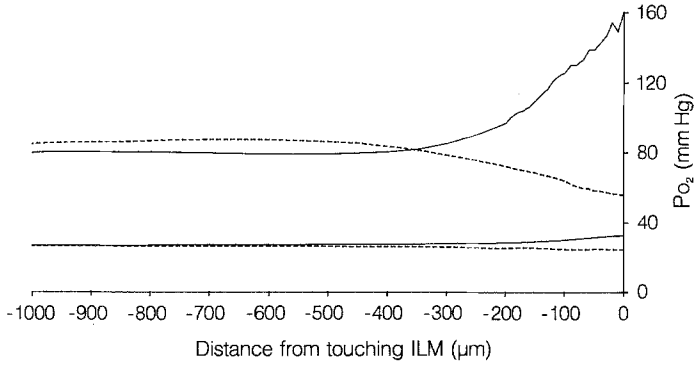

Fig. 3. Vitreal oxygen tension profiles for air breathing *(lower two curves)* and 100% oxygen breathing *(upper two curves)* in a streptozotocin diabetic rat from the STZ (N) group. Oxygen tension (PO_2) in mm Hg is plotted as a function of distance in μm from the retinal surface, from a retinal artery *(full line)*, and vein *(dashed line)*. ILM = Internal limiting membrane

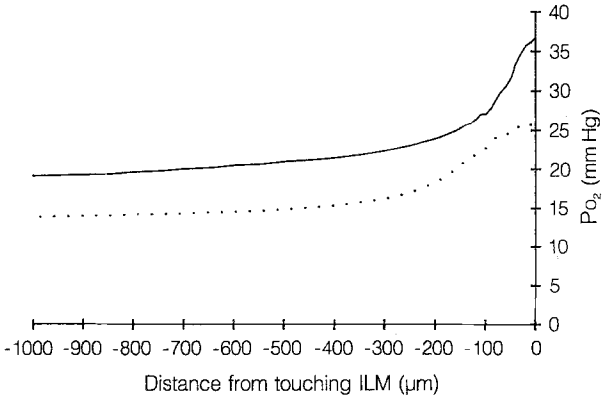

Fig. 4. Two vitreal oxygen tension (PO_2) profiles measured at the same touching artery location in a control rat are compared in normoxia and hypoxia: 20% O_2 (full line), 10% O_2 (dotted line). PO_2 in mm Hg falls as inspired percentage oxygen is decreased but gradients near the retinal artery are maintained. ILM = Internal limiting membrane

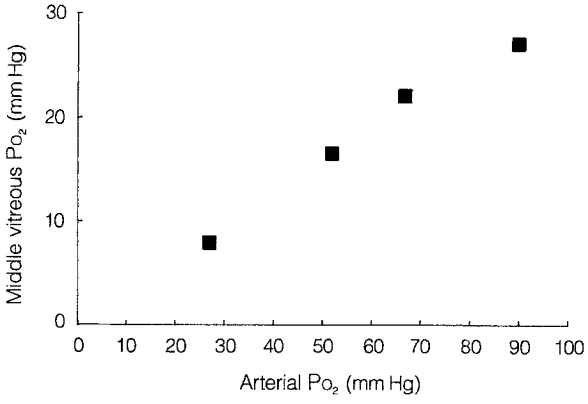

Fig. 5. Relationship of mid vitreal oxygen tension (PO_2) in mm Hg as a function of arterial PO_2 in mm Hg, for one control rat

value which is higher than for air breathing, but in all cases the mid vitreal PO_2 was greater than touching venous PO_2. These results are representative for all those obtained for the STZ (N) rats.

Because the arterial PO_2 for air breathing was significantly lower in the STZ (H) group than in the control group we investigated the effect of acute hypoxia on the control rats in three experiments. Arterial PO_2 was reduced by lowering inspired oxygen concentration and making measurements of arterial blood gases and vitreal PO_2 profiles for each ventilation condition. Two of the resulting arterial PO_2 profiles for one animal are displayed for the ventilation conditions, 20% O_2 and 10% O_2 in Figure 4. The arterial touching PO_2 and mid vitreal PO_2 values fall with the reduction in inspired oxygen. Although all PO_2 values fall, the PO_2 gradients close to the retinal artery are still evident and the A/MV and A/V ratios and arteriovenous oxygen tension difference are higher than those for both groups of STZ rats. Thus, lowering inspired oxygen does reduce vitreal oxygen tension but does not eliminate PO_2 gradients and the arteriovenous oxygen tension difference. The venous and intermediate PO_2 profiles for these two ventilation conditions are omitted to avoid confusing overlap.

The relationship between systemic arterial PO_2 and the resulting mid vitreal PO_2 is plotted in Figure 5 for one of these control animals. This graph demonstrates the direct relationship between these parameters. Indeed, for a mean systemic arterial PO_2 equal to that found in the STZ (H) rats of 58 mm Hg (Table 1) it can be seen that a vitreal PO_2 of just less than 20 mm Hg would be expected, a value which is close to that of the measured mean value of 20.4 mm Hg (Table 2).

Discussion

The data presented in this paper clearly demonstrate that as early as 5–6 weeks after diabetes is induced by an injection of STZ, oxygen tension distribution in the rat vitreous differs from that of the control rat. The vitreal PO_2 profiles in control rats are characterised by the presence of large PO_2 gradients close to retinal arteries. This flow of oxygen by direct diffusion from arteries probably provides the mechanism for supplying oxygen to neural tissue located in the capillary free zone [31] adjacent to retinal arteries and arterioles. The normal rat retinal circulation has a significant arteriovenous oxygen tension difference and a plateau mid vitreal value. This mid vitreal PO_2 is always very close to touching venous PO_2 [32]. These features are very similar to those previously measured for the Wistar rat [32], the cat [33, 34], and the miniature pig [35, 36]. We have previously demonstrated that if the ventilation oxygen percentage is increased to 100%, all vitreal PO_2 values increase in the rat [32, 37], with a marked steepening of oxygen gradients close to the retina, particularly at arteries, so that the arteriovenous oxygen tension difference is increased. In this respect the rat behaves similarly to the cat [33, 34] but differs from the miniature pig [35, 36] which shows no increase in intermediate location PO_2 with hyperoxia.

In the STZ rats we have demonstrated greatly reduced oxygen gradients in the vicinity of retinal arteries. These differences were initially confounded by the problem of attaining normal blood gas values in the STZ group. Using the standard nomogram for setting respiratory parameters for artifically ventilated rats by choosing tidal volume according to body weight, the rats were hypoxic and hypercapnic (STZ [H]). It is apparent that although STZ rats have a low body weight they require a similar respiratory minute volume to that of their control group in order to achieve normal blood gases and blood pH (STZ [N]). This raises the question of whether the rats had the same respiratory minute volume as their controls in the cage or whether they were chronically hypoxic. This is a difficult question to answer. We partially addressed this problem by taking blood samples from a few control and STZ rats during the initial surgery whilst the animals were self-ventilating. There was no apparent difference between the blood gas values for the controls and STZ rats in this condition. It is most likely that the respiratory minute volume for self-ventilating STZ rats is greater than their body weight would suggest. The fact that with artificial ventilation it was never necessary to breathe the STZ rats on a hyperoxic mixture to achieve normal blood gas values implies that normal blood gases are achievable by ventilation adjustments in the self-breathing STZ rat. Low and Tuck have reported normal blood gas levels in their spontaneously breathing STZ rats [38].

Our STZ rats have therefore been subdivided into two groups, those with systemic hypoxia STZ (H), and those which were ventilated with an increased tidal volume to create systemic conditions more equivalent to the control rats STZ (N). The latter group obviously allows the most valuable direct comparison with the control group. The important observation in the STZ (N) group was that although the systemic arterial oxygen tension and mid vitreal oxygen tension were the same as those of the control group the vitreal PO_2 gradients from arteries and the arteriovenous oxygen tension difference were reduced (Figs. 1 b, 2, and Table 2). If the rat is ventilated with 100% O_2, vitreal PO_2 gradients do become evident (Fig. 3) together with a larger arteriovenous oxygen tension difference. Mid vitreal PO_2 now lies between touching arterial and venous PO_2. In this sense the STZ (N) rat PO_2 profiles in hyperoxia are qualitatively similar to those of the control rats. We do not have sufficient data in hyperoxia to determine whether there are any quantitative differences between the control and STZ (N) groups in hyperoxia.

The observation that mid vitreal PO_2 in the rat is not changed in diabetes agrees with previous measurements of vitreal PO_2 in the pancreatectomised cat after 5–12 months of hyperglycaemia [39]. However, the loss of arterial PO_2 gradients and a reduced arteriovenous oxygen tension difference has not been reported before as no other study has examined the oxygen distribution adjacent to retinal vessels in diabetes.

What are the implications of these data? As the absolute values of mid vitreal PO_2 do not differ in the control and STZ (N) groups, then touching arterial PO_2 must be less in the STZ (N) group. As there was no significant difference between arterial blood gases between the control, and STZ (N) groups, therefore a lower systemic arterial PO_2 cannot be the explanation for the reduced oxygen tension adjacent to the retinal artery.

One possible explanation is that diffusion of oxygen from arteries is increased in STZ-induced diabetes, so that although systemic PO_2 is normal, by the time the blood reaches the eye much of the oxygen may have already diffused across the vessel walls. There would not be an equivalent impact on venous PO_2 as this is buffered considerably by the oxyhaemglobin dissociation curve. Thus, by this possible mechanism of increased diffusion from pre-ocular arteries, the retinal arterial oxygen tension and the arteriovenous oxygen tension difference could be reduced. Microsphere studies of retinal blood flow in the alloxan dog model after 6 months of hyperglycaemia revealed a significant reduction in retinal blood flow [40]. Any reduction in flow would presumably increase the oxygen losses in transit to the eye. There is also recent contradictory evidence of increased blood flow in the retina and uvea in STZ rats, again using microsphere techniques [41].

An alternative explanation involves the opposite possibility, namely, that in the diabetic retina there is a diffusion barrier to oxygen developed between the vessel lumen and outside the vessel in the vitreous where the measuring electrode is positioned. This would mean that diffusion of

oxygen from the vessel is reduced and that the oxygen microelectrode is not reflecting intra-luminal PO_2. In this situation intra-luminal PO_2 could be normal, but our measurement made by touching the outside of the artery would be reduced. A factor to be considered in both cases is the possibility of altered oxygen diffusion and solubility properties in the vitreous in diabetes. Thus, one explanation requires increased leakiness to oxygen and the other a reduced leakiness.

There is an increasing body of evidence that diffusion of oxygen from arterioles as well as capillaries plays a major role in oxygenating tissue. Indeed it has been estimated that 2/3 of all oxygen comes from arterioles rather than capillaries in the hamster retractor muscle [42]. The capillary free zone of the retina attests to this oxygenation mechanism existing in the retina, indeed it may be that the superficial retinal layers are largely provided with oxygen by this mechanism whereas the deeper layers rely more on the release of oxygen from erythrocytes in the capillaries.

The observation of a pinker appearance of the retina in the STZ rats may reflect an increased erythrocyte haematocrit in the microcirculation. It may be that the ratio of erythrocyte to plasma perfusion distribution has increased in the STZ rat. There is certainly evidence for heterogeneity of erythrocyte perfusion through the retinal microcirculation in the normal retina from in vivo microscopy studies [43].

In the other diabetic group, the STZ (H) rats, systemic hypoxia plus diabetes resulted in an almost complete loss of arterial PO_2 gradients (Figs. 1 c and 2) whereas making a control rat hypoxic to the same extent (Fig. 4) did not result in a loss of gradient although mid vitreous PO_2 was less in both cases. Thus, the loss of vitreal PO_2 gradients appears to be a feature of the diabetes and not a consequence of systemic hypoxia. At present, any explanation of the mechanisms responsible for these results remains speculative. Further interpretation would certainly be facilitated by measurements of retinal blood flow, intraretinal oxygen tension profiles, and an electrophysiological assessment of retinal function in control and STZ rats.

There is supporting evidence from other tissues for alterations in blood flow accompanying tissue oxygen tension changes in diabetes. In the STZ diabetic kidney, renal blood flow and autoregulatory capacity has been shown to be reduced within 4–5 weeks after the onset of hyperglycaemia [44, 45]. This reduction in blood flow also occurs in peripheral nerve with an accompanying reduction in tissue oxygen tension [38, 46]. In contrast, in cerebral cortex the arterioles have been shown to have a larger lumen, an increased resting blood flow with an accompanying rise in tissue PO_2 in STZ diabetic rats 8–10 weeks post-injection [47]. Also, there is evidence from microsphere measurements of blood flow in the STZ rat that after 6 weeks of hyperglycaemia retinal blood flow has increased by 20% and posterior uveal blood flow by 70% [41]. Resting arteriolar vasodilation has also been observed in the mesenteric arteries of STZ rats after only 4–5 weeks of diabetes which occurs with a reduced wall to lumen ratio [48].

At this stage of STZ diabetes in the rat however there is no evidence for the commonly cited pathological changes to the retinal vasculature seen later. For some rats we compared whole mounted trypsin digests of the retinal vasculature for control and STZ rats and were unable to detect any changes in endothelial cells, pericytes, capillary density or diameter, 5–6 weeks after the onset of hyperglycaemia. Cameron et al., [49] also found no basement thickening after 4 weeks of STZ diabetes. Thus, these alterations in retinal oxygen tension distribution near retinal arteries represents an early change in STZ diabetes before histological changes become apparent.

Relevant animal models of diabetic retinopathy are essential if we are to understand the sequence of pathological events in the disease. The advanced stages of background and proliferative retinopathy have only been demonstrated in the alloxan diabetic dog [50], and not in the streptozotocin-induced monkey and rat [51, 52]. However, the earliest microangiopathic changes which characterise human diabetic retinopathy have also been demonstrated in alloxan induced and spontaneously diabetic dogs [6, 7, 50] and the galactosaemic and STZ-induced and the spontaneously diabetic rat [4, 5, 8, 9], and in the STZ-induced monkey [51]. The STZ rat, in which the microangiopathy develops at an accelerated rate represents a valuable model for investigating the earliest pathology. Using this model we present the first evidence that within 5 weeks of the onset of hyperglycaemia after induced STZ diabetes there are significant changes in the oxygen distribution in the vitreous. The implications of these data for human diabetes remains to be determined.

Acknowledgements. The authors wish to acknowledge the assistance of Mr. M. J. Brown with all aspects of the experiments, Mr. W. Brewster for the design and the manufacture of modifications to the stereotaxic frame, Mr. L. Aravena for the manufacture of the plano concave contact lens, and Mr. D. Heliums for care of the rat colony. We thank Byk Gulden for the gift of Inactin. This research was supported by the Juvenile Diabetes Foundation International, the Medical Research Fund of Western Australia, the Ophthalmic Research Institute of Australia, the Juvenile Diabetes Foundation of Australia, TVW Telethon, the Clive and Vera Ramaciotti Foundations, and the National Health and Medical Research Council of Australia.

References

1. Kuwabara T, Cogan DG (1960) Studies of retinal vascular patterns. Arch Ophthalmol 64: 904–911
2. Toussaint D, Kuwabara T, Cogan DG (1961) Retinal vascular patterns 2. Human retinal vessels studied in three dimensions. Arch Ophthalmol 65: 137–143
3. Cogan DG, Toussaint D, Kuwabara T (1961) Retinal vascular patterns 4. Diabetic retinopathy. Arch Ophthalmol 66: 100–112
4. Waber S, Meister V, Rossi GL, Mordasini R-C, Riesen WF (1981) Studies on retinal microangiopathy and coronary macroangiopathy in rats with streptozotocin-induced diabetes. Virch Arch (Cell Path) 37: 1–10
5. Robison WG, Nagata M, Laver N, Hohman T, Kinoshita JH (1989) Diabetic-like retinopathy in rats prevented with an aldose reductase inhibitor. Invest Ophthalmol Vis Sci 30: 2285–2292
6. Engerman RL, Finkelstein D, Aquirre G (1982) Animals appropriate for studying diabetes mellitus and its complications: ocular complications. Diabetes 31 [Suppl. 1]: 82–88
7. Engerman RL, Kern TS (1984) Experimental galactosemia produces diabetic-like retinopathy. Diabetes 33: 97–100
8. Papachristodoulou D, Heath H, Kang SS (1976) The development of retinopathy in sucrose-fed and streptozotocin-diabetic rats. Diabetologia 12: 367–374

9. Cameron DP, Amherdt M, Leuenberger P, Orci L, Stauffacher W (1973) Microvascular alterations in chronically streptozotocin-diabetic rats. Adv Metab Disord [Suppl. 2]: 257–269
10. Cunha-Vaz JG, Gray JR, Zeimer RC, Mota MC (1985) Characterisation of the early stages of diabetic retinopathy by vitreous fluorophotometry. Diabetes 34: 53–59
11. Kaufman F, Lacoste C (1986) Vitreous fluorescein accumulation determined by in vivo fluorophotometry and by vitreous extraction in normal and diabetic rats. Diabetologia 29: 175–180
12. Vine AK, Kisby AM, Betz AL, Howatt WF (1984) Vitreous fluorophotometry in rats with streptozotocin-induced diabetes. Arch Ophthalmol 102: 1083–1085
13. Vinores SA, Campochiaro PA, May EE, Blaydes SH (1988) Progressive ultrastructural damage and thickening of the basement membrane of the retinal pigment epithelium in spontaneously diabetic BB rats. Exp Eye Res 46: 545–558
14. Caldwell RB, Slapnick SM, McLaughlin BJ (1986) Decreased anionic sites in Bruchs Membrane area of the retinal pigment epithelium in experimental diabetes. Invest Ophthalmol Vis Sci 27: 1691–1697
15. Grimes PA, McGlinn A, Laties AM, Naji A (1984) Increase of basal cell membrane area of the retinal pigment epithelium in experimental diabetes. Exp Eye Res 38: 569–577
16. Cunha-Vaz J, De Abreu F, Campos AJ (1975) Early breakdown of the blood retinal barrier in diabetes. Br J Ophthalmol 59: 649–656
17. Ditzel J, Standl E (1975) The problem of tissue oxygenation in diabetes 2. Evidence of disordered oxygen release from erythrocytes of diabetics in various conditions of metabolic control. Acta Med Scand [Suppl.] 578: 59–83
18. Hoare EM, Barnes AJ, Dormandy JA (1976) Abnormal blood viscosity in diabetes mellitus and retinopathy. Bioreheol 13: 21–25
19. Pedizzi M, Melli M, Fonda S, Codeluppi L, Guerrier F (1984) Comparative evaluation of blood viscositiy in diabetic retinopathy. Int Ophthalmol 7: 15–19
20. Macmillan D, Utterback N, La Puma JL (1976) Reduced erythrocyte deformability in diabetes. Diabetes 27: 895–901
21. Benarroch S, De Salama R, Bregni C (1989) Correction of blood hyperviscosity in diabetes with microangiopathy by hematocrit reduction (therapeutic implications). Clin Hemorheol 9: 559–568
22. Ben-Nun J, Alder VA, Constable IJ, Roberts CE (1990) The patency of the retinal vasculature to erythrocytes in retinal vascular disease. Invest Ophthalmol Vis Sci 31: 464–470
23. Grunwald JE, Riva CE, Brucker AJ, Sinclair SH, Petrig BL (1984) Altered retinal vascular response to 100% oxygen breathing in diabetes mellitus. Ophthalmology 91: 1447–1452
24. Rimmer T, Fallon TJ, Kohner EM (1989) Long term follow up of retinal blood flow in diabetics using the blue field entoptic phenomenon. Br J Ophthalmol 73: 1–5
25. Blair NP, Riva CE (1982) Prolongation of the retinal mean circulation time in diabetes. Arch Ophthalmol 100: 764–768
26. Grunwald JE, Riva CE, Sinclair SH, Brucker AJ, Benno LP (1986) Laser doppler velocimetry study of retinal circulation in diabetes mellitus. Arch Ophthalmol 104: 991–996
27. Kleinman L, Radford EP Jr (1988) Harvard Apparatus Publication 5375-001 Rev 2 H S S
28. Duhling BR, Kuschinsky W, Wahl M (1979) Measurements of the perivascular PO_2 in the vicinity of the pial vessels of the cat. Pflügers Arch 383: 29–34
29. Cutler RWP, Young JN, Urion DK (1983) Factors which influence the vitreous potassium concentration in the rat. Invest Ophthalmol Vis Sci 24: 631–636
30. Chadhuri A, Hallett PE, Parker JA (1983) Aspheric curvatures, refractive indices and chromatic aberration for the rat eye. Vis Res 23: 1351–1364
31. Michaelson IC (1948) The mode of development of the retinal vessels and some observations of its significance in certain retinal diseases. Trans Ophthalmol Soc. U.K. 68: 137–145
32. Alder VA, Yu D-Y, Cringle SJ (1991) Vitreal oxygen tension measurements in the rat eye. Exp Eye Res 52: 293–299
33. Alder VA, Cringle SJ (1985) The effect of the retinal circulation on the vitreal oxygen tension. Curr Eye Res 4: 121–129
34. Alder VA, Cringle SJ (1990) Vitreal and retinal oxygenation. Grafe's Arch Clin Exp Ophthalmol 228: 151–157
35. Pournaras CJ, Riva CE, Tsacopoulos M, Strommer K (1989) Diffusion of O_2 in the retina of anaesthetized miniature pigs in normoxia and hyperoxia. Exp Eye Res 49: 347–360
36. Molnar I, Pointry S, Tsacopoulos M, Giladi N, Leuenberger PM (1985) Effect of laser photocoagulation on oxygenation of the retina in miniature pigs. Invest Ophthalmol Vis Sci 26: 1410–1414
37. Yu D-Y, Cringle SJ, Alder VA (1990) The response of rat vitreal oxygen tension to stepwise increases in inspired oxygen tension. Invest Ophthalmol Vis Sci 31: 2493–2499
38. Tuck RR, Schmelzer JD, Low PA (1984) Endoneurial blood flow and oxygen tension in the sciatic nerves of rats with experimental diabetic neuropathy. Brain 107: 935–950
39. Stefansson E, Hatchell DL, Fischer BL, Sutherland FC, Machemer R (1986) Panretinal photocoagulation and retinal oxygenation in normal and diabetic cats. Am J Ophthalmol 101: 657–664
40. Small KW, Stefansson E, Hatchel DL (1987) Retinal blood flow in normal and diabetic dogs. Invest Ophthalmol Vis Sci 28: 672–675
41. Tilton RG, Chang K, Pugliese G, Eades DM, Province MA, Sherman WR, Kilo C, Williamson JR (1989) Prevention of hemodynamic and vascular albumin filtration changes in diabetic rats by aldose reductase inhibitors. Diabetes 38: 1258–1270
42. Pittman RN (1987) Oxygen delivery and transport in the microcirculation, In: McDonagh PF (ed) Microvascular perfusion and transport in health and disease. Karger, Basel, pp 60–79
43. Thuranzky K (1957) Der Blutkreislauf der Netzhaut. Intravitalmikroskopische und Histologische Studien an der Katzenretina, Verlag der Ungarischen Akademie der Wissenschaften, Budapest
44. Hashimoto Y, Ideura T, Yoshimura A, Koshikawa S (1989) Autoregulation of renal blood flow in streptozotocin-induced diabetic rats. Diabetes 38: 1109–1113
45. Ha H, Dunham EW (1987) Limited capacity for renal vasodilation in anaesthetised diabetic rats. Am J Physiol 253: H854–H855
46. Newrick PG, Wilson AJ, Jakubowski J, Boulton AJM, Ward JD (1986) Sural nerve oxygen tension in diabetes. Br Med J 293: 1053–1054
47. Rubin MT, Bohlen HG (1985) Cerebral vascular autoregulation of blood flow and tissue PO_2 of diabetic rats. Am J Physiol 249: H540–H546
48. Bohlen HG, Hankins KD (1966) Early arteriolar and capillary changes in streptozotocin-induced diabetic rats and intraperitoneal hyperglycaemic rats. Diabetologia 22: 344–348
49. Cameron DP, Amherdt M, Leuenberger P, Orci L, Stauffacher W (1973) Microvascular alterations in chronically streptozotocin-diabetic rats. Adv Metab Disord [Suppl. 2] 257–269
50. Engerman RL, Kramer JW (1982) Dogs with induced or spontaneous diabetes as models for the study of human diabetes mellitus. Diabetes 31: 26–29
51. Tso MOM (1985) A review: diabetic retinopathy – pathophysiologic and therapeutic approaches. Drug Develop Res 6: 217–233
52. Jonasson O, Jones CW, Baumann A, John E, Manaligod J, Tso MOM (1985) The pathophysiology of experimental insulin-deficient diabetes in the monkey. Ann Surg 201: 27–39

Received: 27 December 1990
and in revised form: 19 March 1991

Dr. V. Alder
Lions Eye Institute
2 Verdun Street
Nedlands 6009
Western Australia
Australia